

# Blocking endothelin-1-receptor/ $\beta$ -catenin circuit sensitizes to chemotherapy in colorectal cancer

Roberta Cianfrocca<sup>1</sup>, Laura Rosanò<sup>1</sup>, Piera Tocci<sup>1</sup>, Rosanna Sestito<sup>1</sup>, Valentina Caprara<sup>1</sup>, Valeriana Di Castro<sup>1</sup>, Ruggero De Maria<sup>2</sup> and Anna Bagnato<sup>\*,1</sup>

The limited clinical response to conventional chemotherapeutics observed in colorectal cancer (CRC) may be related to the connections between the hyperactivated  $\beta$ -catenin signaling and other pathways in CRC stem-like cells (CRC-SC). Here, we show the mechanistic link between the endothelin-1 (ET-1)/ET-1 receptor (ET-1R) signaling and  $\beta$ -catenin pathway through the specific interaction with the signal transducer  $\beta$ -arrestin1 ( $\beta$ -arr1), which initiates signaling cascades as part of the signaling complex. Using a panel of patient-derived CRC-SC, we show that these cells secrete ET-1 and express ET<sub>A</sub>R and  $\beta$ -arr1, and that the activation of ET<sub>A</sub>R/ $\beta$ -arr1 axis promotes the cross-talk with  $\beta$ -catenin signaling to sustain stemness, epithelial-to-mesenchymal transition (EMT) phenotype and response to chemotherapy. Upon ET<sub>A</sub>R activation,  $\beta$ -arr1 acts as a transcription co-activator that binds  $\beta$ -catenin, thereby promoting nuclear complex with  $\beta$ -catenin/TFC4 and p300 and histone acetylation, inducing chromatin reorganization on target genes, such as ET-1. The enhanced transcription of ET-1 increases the self-sustained ET-1/ $\beta$ -catenin network. All these findings provide a strong rationale for targeting ET-1R to hamper downstream  $\beta$ -catenin/ET-1 autocrine circuit. Interestingly, treatment with macitentan, a dual ET<sub>A</sub>R and ET<sub>B</sub>R antagonist, able to interfere with tumor and microenvironment, disrupts the ET-1R/ $\beta$ -arr1- $\beta$ -catenin interaction impairing pathways involved in cell survival, EMT, invasion, and enhancing sensitivity to oxaliplatin (OX) and 5-fluorouracil (5-FU). In CRC-SC xenografts, the combination of macitentan and OX or 5-FU enhances the therapeutic effects of cytotoxic drugs. Together, these results provide mechanistic insight into how ET-1R coopts  $\beta$ -catenin signaling and offer a novel therapeutic strategy to manage CRC based on the combination of macitentan and chemotherapy that might benefit patients whose tumors show high ET<sub>A</sub>R and  $\beta$ -catenin expression.

*Cell Death and Differentiation* (2017) 24, 1811–1820; doi:10.1038/cdd.2017.121; published online 14 July 2017

Colorectal cancer (CRC) is one of the main causes of tumor-related mortality worldwide and its therapy mainly relies on the use of conventional chemotherapeutic drugs.<sup>1</sup> Most CRC carry mutations leading to overactivation of the  $\beta$ -catenin pathway.<sup>2</sup> CRC stem-like cells (CRC-SC) have been shown to be responsible for tumor propagation, metastasis and resistance to conventional anticancer drugs.<sup>3–10</sup> An accurate understanding of the cross-talk between signaling in CRC-SC could allow the development and the clinical use of effective therapies to enhance CRC drug sensitivity. In CRC-SC  $\beta$ -catenin signaling pathway promotes tumor growth, and progression by sustaining stem cell expansion.<sup>11–14</sup> A key property of CRC-SC with activated  $\beta$ -catenin signaling is the protection against conventional chemotherapeutics.<sup>2,15</sup> The molecular mechanisms responsible of the fine-tuning of  $\beta$ -catenin-mediated stemness and drug response remain largely unexplored but represent a potentially promising area for novel therapeutic interventions. Therefore, drugging upstream signaling molecules endowed with functions that regulate  $\beta$ -catenin activity may represent a novel approach to sensitize to chemotherapy. In this context, endothelin-1 (ET-1) elicits pleiotropic effects in tumor cells and in the host microenvironment, modulating the epithelial-to-mesenchymal

transition (EMT), the expansion of vascular network and immune response.<sup>16</sup> ET-1 acts through autocrine and paracrine signaling by binding two distinct receptors: endothelin A (ET<sub>A</sub>R) and B (ET<sub>B</sub>R), which belong to the G-protein-coupled receptor family. The activation of ET-1/ET<sub>A</sub>R axis is recognized as a common mechanism underlying the progression of various solid tumors, including CRC.<sup>16–18</sup> In CRC, the components of the ET-1 system are expressed not only by tumor cells, but also by microenvironmental elements, such as fibroblasts, endothelial cells and macrophages.<sup>17–26</sup> Increased levels of ET-1 have been detected in plasma and tissue samples from patients with CRC.<sup>19,20</sup> Moreover, in CRC the ET-1 gene regulation is directly upregulated by  $\beta$ -catenin.<sup>27</sup> Microarray molecular profiling and real-time PCR on CD133<sup>+</sup> fractions of CRC lines revealed that ET-1 transcripts are highly expressed compared with CD133<sup>-</sup> counterparts.<sup>28</sup> A preclinical study in CRC demonstrated that zibotentan, a selective ET<sub>A</sub>R antagonist, suppressed tumor growth and progression indicating a potential role of this antagonist as adjuvant therapy.<sup>29</sup> More recently in CRC cells, it has been demonstrated that overexpression of the ET-1 gene is a determinant of acquired resistance to MEK and PI3K inhibitors.<sup>30</sup> However

<sup>1</sup>Preclinical Models and New Therapeutic Agents Unit, Regina Elena National Cancer Institute, Rome, Italy and <sup>2</sup>Institute of General Pathology, Catholic University, Rome, Italy

\*Corresponding author: A Bagnato, Preclinical Models and New Therapeutic Agents Unit, Regina Elena National Cancer Institute, Via Elio Chianesi, 53, Rome 00144, Italy. Tel: +39 06 5266 5618; Fax: +39 06 5266 2600; E-mail: annateresa.bagnato@ifo.gov.it

Received 20.3.17; revised 09.6.17; accepted 23.6.17; Edited by G Kroemer; published online 14.7.17

the molecular mechanism of ET-1 axis to protect against drugs treatment in CRC remains elusive.

In our recent studies, we reported that ET-1/ $E_{TA}R$  axis, through the contribution of the scaffold protein  $\beta$ -arrestin1 ( $\beta$ -arr1), appears to be critical in the signaling cross-talk, providing a mechanism of escape to a new less-adverse niche, in which evasion of drug-induced apoptosis ensures cell survival required for tumor progression.<sup>16,31–35</sup> In this regard, ET-1 has been recently identified as a key component that sustains maintenance and clonal expansion of cardiovascular stem cells population.<sup>36</sup> Moreover, a recent report suggests that  $\beta$ -arr1 has an important protective role, reducing the chemotherapy-induced intestinal stem cell apoptosis.<sup>37</sup> To dissect the intricate interplay between ET-1/ $\beta$ -arr1 and  $\beta$ -catenin, here we report a ET-1/ $\beta$ -arr1-mediated epigenetic mechanism in regulating  $\beta$ -catenin signaling to promote EMT and protection against chemotherapy. Understanding whether targeting ET-1/ $\beta$ -arr1 connected with  $\beta$ -catenin pathway in CRC-SC can restore sensitivity to chemotherapy, is thus essential to develop more effective strategies in this malignancy.

## Results

**Expression of ET-1/ $\beta$ -arr1 axis in CRC-SC.** We first evaluated the expression of ET-1 axis in CRC-SC features, by using a panel of patient-derived CRC-SC isolated from human tumor samples (CC09, CSC5, CSC2 and CSC1), all carrying APC gene mutations.<sup>3,10,12</sup> The mRNA and protein expression analysis showed that all CRC-SC expressed ET-1 and its receptors,  $E_{TA}R$  and  $E_{TB}R$ , and released high levels of ET-1, within the physiologically range needed for the activation of ET-1R in an autocrine manner<sup>38</sup> (Figures 1a–c). To explore the role of  $\beta$ -arr1 to create intracellular signaling cross-talk upon ET-1R activation, we first evaluated  $\beta$ -arr1 expression in CRC-SC. These cells expressed  $\beta$ -arr1 both at mRNA and protein levels (Figures 1a and b). After ET-1 stimulation, we observed an increase of CRC-SC viability, which was reduced after treatment with macitentan, a potent  $E_{TA}R$  antagonist with significant affinity for  $E_{TB}R$ . The same effect was observed after  $\beta$ -arr1 silencing (Figure 1d and Supplementary Figure S1a and S2). When cultured in stem cell medium, CRC-SC grow in large round, unattached floating spheroid colonies (sphere). As shown in Figure 1e, whereas the ET-1 addition enhanced the CRC-SC sphere formation ability, increasing not only the sphere number but also the size, macitentan treatment negatively affected the stemness property of CRC-SC, indicating that the ET-1/ $\beta$ -arr1 axis sustains CRC-SC features.

**ET-1/ $\beta$ -arr1-driven EMT and invasive behavior in CRC-SC.** Next, we analyzed whether the features of CRC-SC driven by  $E_{TA}R$ / $\beta$ -arr1 were associated with molecular changes consistent with EMT.<sup>39–44</sup> To this end we examined the expression of the epithelial marker E-cadherin and its transcriptional repressors, Twist and Snail, as well as the expression of mesenchymal markers, such as N-cadherin and vimentin. Upon ET-1 stimulus, we observed an increase of N-cadherin, vimentin, Snail and Twist

expression levels, associated with a concomitant decrease in E-cadherin expression (Figures 2a and b). In addition, as a result of macitentan treatment or  $\beta$ -arr1 silencing, restored E-cadherin expression and inhibited N-cadherin, Snail and Twist expression were observed (Figure 2b). Concordantly, the analysis of mRNA levels upon ET-1 stimulation showed the increased expression levels of Snail and N-cadherin and the decrease of E-cadherin that were reverted following macitentan treatment (Figure 2c). Remarkably, macitentan, or the  $\beta$ -arr1 knockdown, inhibited the ET-1-induced suppression of E-cadherin promoter activity (Figure 2d) and induction of Snail promoter activity (Figure 2e). Next, we evaluated whether the  $E_{TA}R$ / $\beta$ -arr1-driven acquisition of EMT phenotype correlates with expression and activation of the proteolytic enzymes, matrix metalloproteases (MMP), and with an increase of invasive potential of CRC-SC. As shown in Figures 2f and g, the ET-1-induced MMP-2 and -9 secretion and activation were inhibited by macitentan treatment, as well as  $\beta$ -arr1 silencing, as determined by immunoblotting and zymography. In this context, as a result of enhanced proteolytic activity of CRC-SC upon  $E_{TA}R$ / $\beta$ -arr1 signaling activation, when CRC-SC were silenced for  $\beta$ -arr1 or were treated with macitentan, the ET-1-induced cell invasion was significantly impaired compared with control cells (Figure 2h), providing evidence that  $E_{TA}R$ / $\beta$ -arr1 axis activation may be a critical event to drive EMT and invasive behavior in CRC-SC.

**ET-1/ $\beta$ -arr1 axis links  $\beta$ -catenin pathway in CRC-SC.** The  $\beta$ -catenin signaling pathway represents an hallmark of CRC-SC governing the maintenance of stemness.<sup>2,11–15</sup> We observed that ET-1 stimulation induced the  $\beta$ -catenin nuclear translocation, an effect that was inhibited upon macitentan treatment (Figure 3a), enhancing the levels of serine/threonine non-phosphorylated  $\beta$ -catenin active form (Supplementary Figure S3a). We analyzed the nucleocytoplasmic shuttling of both  $\beta$ -arr1 and  $\beta$ -catenin in the cytosolic and nuclear extracts of CRC-SC upon different times of ET-1 stimulation. ET-1 induced a time-dependent nuclear translocation of both proteins with a peak after 30 and 60 min of ET-1 challenge (Figure 3b). Of relevance, this effect was strongly reduced upon macitentan treatment and  $\beta$ -arr1 silencing (Figure 3c). Moreover, we analyzed  $\beta$ -arr1 and  $\beta$ -catenin potential physical interaction in the nucleus, by using co-immunoprecipitation (IP) assays.  $\beta$ -arr1 bound to  $\beta$ -catenin in the nuclei of ET-1-treated cells (Figure 3d), and this interaction was inhibited by macitentan, suggesting that ET-1/ $\beta$ -arr1 links  $\beta$ -catenin in the nucleus of CRC-SC that is hampered by ET-1R blockade. Consistent with these results, the transcriptional activity of  $\beta$ -catenin, induced by ET-1 in CRC-SC, was inhibited after treatment with macitentan, or by  $\beta$ -arr1 silencing (Figure 3e and Supplementary Figure S3b), indicating that ET-1/ $\beta$ -arr1/ $\beta$ -catenin interaction is necessary for inducing  $\beta$ -catenin/T cell factor 4 (TCF4) transcriptional activity. Given that ET-1 is also a downstream target gene of  $\beta$ -catenin/TCF4,<sup>27,31,32</sup> by using a reporter plasmid with ET-1 promoter sequence, containing a functional TCF binding element (TBE), we demonstrated that ET-1 promoter activity was significantly upregulated after ET-1 stimulation and inhibited when the cells were treated with macitentan, or silenced for  $\beta$ -arr1 (Figure 3f). Next, through

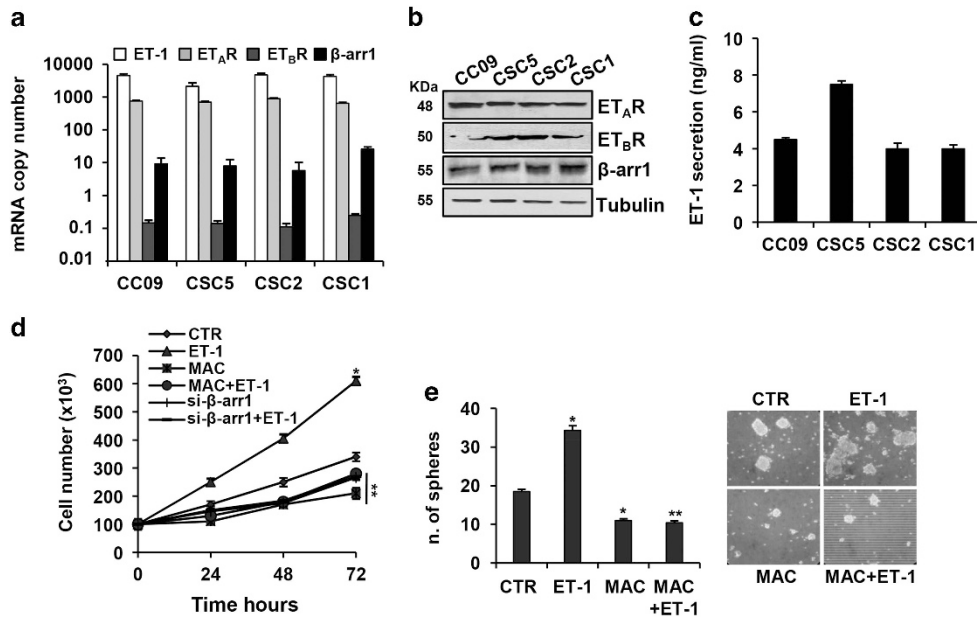


**Figure 1** Expression of ET-1/ $\beta$ -arr1 axis in CRC-SC. (a) In a panel of patient-derived CRC-SC (CC09, CSC5, CSC2 and CSC1), expression of ET-1, ET<sub>A</sub>R, ET<sub>B</sub>R and  $\beta$ -arr1 mRNA copy number was analyzed by real-time PCR (qPCR) normalized using endogenous cyclophilin-A. Values are shown as mean  $\pm$  S.D. from three independent experiments repeated in triplicates. (b) ET<sub>A</sub>R, ET<sub>B</sub>R and  $\beta$ -arr1 protein expression was analyzed by immunoblotting (IB). Tubulin was used as loading control. (c) ET-1 secretion evaluated by ELISA in 24 h cell-conditioned media. Values are shown as mean  $\pm$  S.D. from three independent experiments repeated in triplicates. (d) Time-dependent effect of treatment with ET-1 (100 nM) and/or macitentan (MAC) (1  $\mu$ M) on cell growth of CC09 cells transfected with siRNA negative control (SCR) or with  $\beta$ -arr1 siRNA (si- $\beta$ -arr1). Values are shown as mean  $\pm$  S.D. from three independent experiments repeated in triplicates (\* $P$  < 0.001 versus CTR; \*\* $P$  < 0.001 versus ET-1) (e) Sphere formation assay of CSC5 cells, treated with ET-1 (100 nM) and MAC (1  $\mu$ M) alone or in combination for 7 days. Values are shown as mean  $\pm$  S.D. from three independent experiments repeated in triplicates (\* $P$  < 0.05 versus CTR; \*\* $P$  < 0.05 versus ET-1). Representative images of tumor spheres were shown in the right panel

chromatin immunoprecipitation (ChIP) assays, we demonstrated that in CRC-SC, both  $\beta$ -arr1 and  $\beta$ -catenin, together with TCF4, were recruited on TBE of ET-1 promoter. In parallel, ET-1 stimulation induced the acetylation of histone 3 at Lysine 27 (H3K27), and the competent recruitment of p300 together with  $\beta$ -arr1 and  $\beta$ -catenin (Figures 3g and h). Knocking down of  $\beta$ -arr1 or treatment with macitentan abolished the ET-1-induced effect (Figures 3g and h). Hence, in response to ET-1R activation,  $\beta$ -arr1 was selectively enriched with  $\beta$ -catenin on ET-1 promoter and the cooperation between these two proteins enhanced the autoregulatory  $\beta$ -catenin-mediated transcription of ET-1 gene. In parallel, we evaluated the influence of the ET-1 axis activation on the transcription of a set of specific  $\beta$ -catenin/TCF4-target genes, such as ET-1, Cyclin D1 and Axin 2. As shown in Figure 3i, the analysis of mRNA showed an upregulation of the levels of these genes upon ET-1 stimulation, and a considerable decrease after macitentan treatment. Collectively, our findings highlight the role of ET-1R/ $\beta$ -arr1 signaling to interconnect the  $\beta$ -catenin pathway in CRC-SC, to form specific nuclear complex that regulates histone acetylation in specific chromosomal regions, upregulating the transcription of different  $\beta$ -catenin target genes, including the self-sustained ET-1/ $\beta$ -catenin activity, as a magnifying mechanism.

**ET-1R blockade sensitizes CRC-SC to standard chemotherapeutic drugs.** In CRC-SC, ET-1R/ $\beta$ -arr1 modulates cell survival pathways. Thus, the stimulation of CRC-SC with ET-1 was accompanied with phosphorylation of both p42/

p44MAPK and Akt, and macitentan treatment, or the specific  $\beta$ -arr1 silencing, significantly decreased the ET-1-mediated MAPK and Akt activation (Figure 4a and Supplementary Figure S4a). Because a typical property of CRC-SC is the resistance to treatment with standard chemotherapeutic agents, as oxaliplatin (OX) and 5-fluorouracil (5-FU), we evaluated the response of CRC-SC following exposure to OX and 5-FU at clinically relevant doses,<sup>10</sup> and found that these cells were poorly responsive to chemotherapeutic drugs-induced apoptosis even at the highest concentration used (Figure 4b). The treatment with macitentan or the loss of  $\beta$ -arr1 in a combination regimen with OX or 5-FU, induced a more effective reduction of cell vitality (Figure 4c and Supplementary Figure S4b). Furthermore, CRC-SC that overexpressed exogenous  $\beta$ -arr1-FLAG showed a greater poor sensitivity to OX or 5-FU, compared with parental cells (Figure 4d and Supplementary Figure S1b), suggesting that ET<sub>A</sub>R/ $\beta$ -arr1 blockade might sensitize CRC-SC to OX and 5-FU-induced apoptosis. Mechanistically, we found that the combined treatment of macitentan with chemotherapeutic agents, resulted in an enhanced expression of the poly ADP-ribose polymerase (PARP) cleaved form (Figure 4e and Supplementary Figure S4c). In addition, we found that ET-1 increased the expression of the prosurvival factor Bcl-XL, which was strongly reduced upon macitentan and OX co-treatment (Figure 4f). This implies that the activation of ET-1R/ $\beta$ -arr1 survival signaling is involved in the protection of CRC-SC against chemotherapeutics, suggesting that



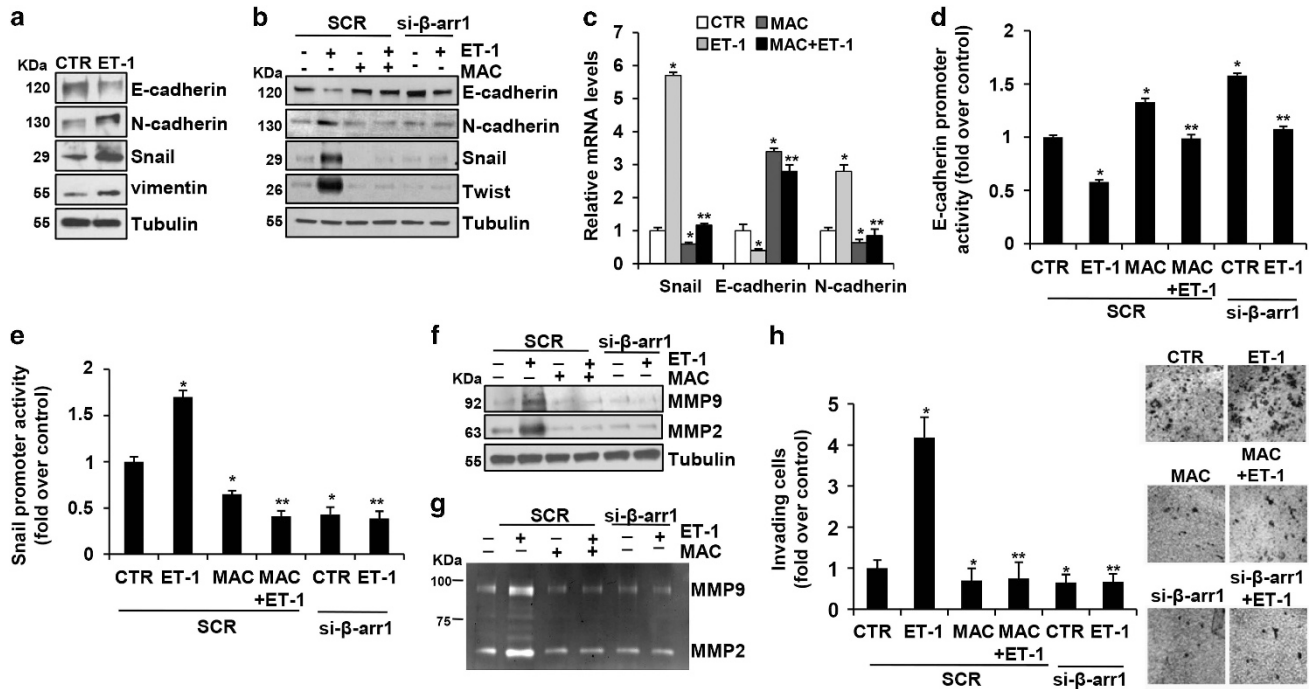


**Figure 2** ET-1R/ $\beta$ -arr1 axis drives EMT process in CRC-SC. (a) Lysates from CCR9 cells were analyzed by IB for the expression of epithelial (E-cadherin) and mesenchymal (N-cadherin, Snail, and vimentin) markers after ET-1 (100 nM) stimulation for 24 h. Tubulin was used as loading control. (b) Lysates from CCR9 cells transfected with SCR or si- $\beta$ -arr1 and treated for 24 h with ET-1 (100 nM) and/or MAC (1  $\mu$ M) were analyzed by IB for the expression of E-cadherin, N-cadherin, Snail and Twist. Tubulin was used as loading control. (c) Snail, E-cadherin, and N-cadherin expression in CCR9 cells upon ET-1 (100 nM) and/or MAC (1  $\mu$ M) treatment evaluated by qPCR, normalized using endogenous cyclophilin-A. Values are shown as mean  $\pm$  S.D. from three independent experiments repeated in triplicates (\* $P$ <0.002 versus CTR; \*\* $P$ <0.005 versus ET-1). (d) E-cadherin promoter activity and Snail promoter activity (e) evaluated in CCR9 cells transfected with SCR or si- $\beta$ -arr1 and treated for 24 h with ET-1 (100 nM) and/or MAC (1  $\mu$ M). Values are shown as mean  $\pm$  S.D. from three independent experiments repeated in triplicates (\* $P$ <0.01 versus CTR; \*\* $P$ <0.001 versus ET-1 in SCR-transfected cells). (f) Lysates from CCR9 cells transfected with SCR or si- $\beta$ -arr1 treated with ET-1 (100 nM) and/or MAC (1  $\mu$ M) for 24 h were analyzed for MMP-2 and -9 by IB. Tubulin was used as loading control. (g) Conditioned media collected from CCR9 treated as in (f) were used to determine the secretion and activity of MMP-2 and -9 by gelatin zymography. (h) Cell invasion assay of CCR9 cells transfected with SCR or si- $\beta$ -arr1 and exposed to ET-1 (100 nM) and/or MAC (1  $\mu$ M) for 24 h. Values are shown as mean  $\pm$  S.D. from three independent experiments repeated in triplicates (\* $P$ <0.002 versus CTR; \*\* $P$ <0.001 versus ET-1 in SCR-transfected cells). Representative images of invading cells were shown in the right panel

molecular targeting of ET-1R in CRC-SC might improve the efficacy of chemotherapeutic regimens.

**ET-1R blockade inhibits tumor growth and restores sensitivity to chemotherapy in CRC-SC patient-derived xenografts.** To verify whether ET-1R blockade by macitentan would also affect tumor growth *in vivo*, patient-derived CCR9 and CSC5 CRC-SC were injected into the flank of mice and were allowed to grow until they reached a detectable size. The xenografts obtained were confirmed as colorectal adenocarcinoma, as showed by hematoxylin–eosin staining in the representative sections from tumor xenografts (Figure 5a and Supplementary Figure S5a). Next, we tested the effect of macitentan alone or in combination with chemotherapy in CRC-SC xenografts. After the appearance of palpable tumors (day 14 for CCR9 xenografts, and day 42 for CSC5 xenografts), mice were randomized into different groups of ten mice undergoing the following treatments for 4 weeks: (i) vehicle (control), (ii) macitentan (30 mg/Kg/oral daily), (iii) OX (0.25 mg/Kg/i.p. once a week) or 5-FU (15 mg/Kg/i.p. daily), (iv) macitentan plus OX or 5-FU. These treatments, were generally well tolerated without any loss of weight or detectable signs of acute or delayed toxicity. At the end of 4 weeks of treatment, tumor size of mice treated with macitentan significantly decreased compared with

vehicle-treated mice (~60% for CCR9 xenografts; 55% for CSC5 xenografts,  $P$ <0.02), demonstrating the therapeutic potential of macitentan in controlling tumor growth. Most importantly, a synergistic growth-inhibitory effect, as calculated by Chou and Talalay method, was observed when macitentan was used in combination with OX, compared with macitentan- or OX-treated mice (90 versus 68% or 12% respectively, for CCR9; 84 versus 55% or 49% respectively, for CSC5 xenografts;  $P$ <0.05) or in combination with 5-FU compared with macitentan- or 5-FU-treated mice (91 versus 50% or 10% respectively, for CCR9 xenografts;  $P$ <0.05, Figure 6), thus proving the ability of macitentan to sensitize CRC-SC xenografts to different chemotherapeutic drugs. Moreover, the therapeutic effects of macitentan were long-lasting, both in monotherapy or combination with chemotherapeutic drugs, for up to 2/3 weeks after termination of treatments. Indeed, we still found a persisted tumor growth reduction even during the treatment-free period in mice treated with macitentan compared with vehicle-treated mice (46% at day 63, for CCR9 xenografts, Figure 5a; 40% at day 55 for CCR9 xenografts, Figure 6; 61% at day 77 for CSC5 xenografts, Supplementary Figure S5a;  $P$ <0.02), and a persistent synergistic inhibitory effect in combinatorial regimes (91 versus 46% for macitentan or 37% for OX, for CCR9 xenografts; 89 versus 40% for

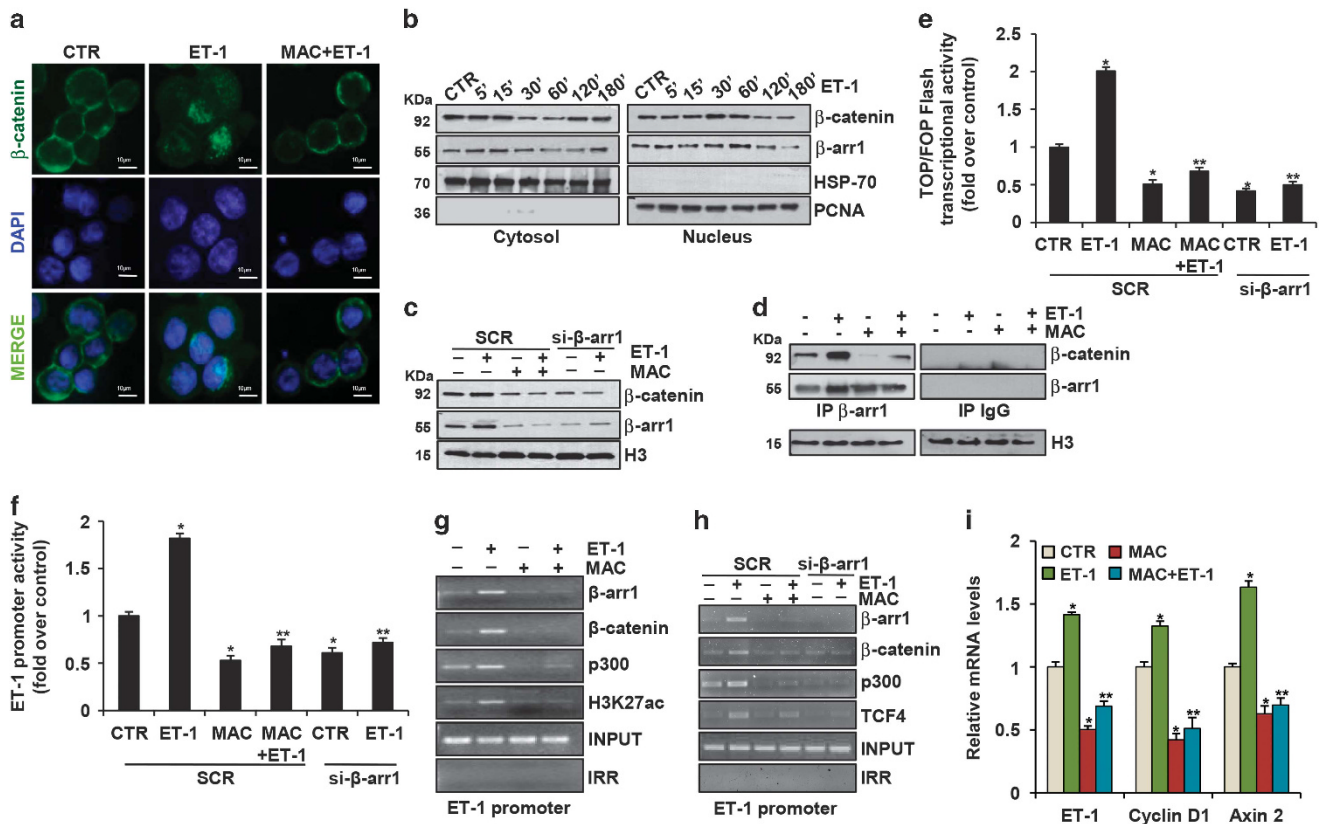


**Figure 3** ET-1R/ $\beta$ -arr1 axis induces  $\beta$ -catenin pathway in CRC-SC. (a)  $\beta$ -catenin localization evaluated by immunofluorescence staining (green) in CC09 cells stimulated for 30 min with ET-1 (100 nM) alone or in combination with MAC (1  $\mu$ M). Nuclei were counterstained with DAPI (blue) (scale bar, 10  $\mu$ m). (b) IB analysis for  $\beta$ -catenin and  $\beta$ -arr1 protein expression in cytoplasmic and nuclear extract of CC09 cells treated with ET-1 (100 nM) for the indicated times. HSP-70 and PCNA were used as cytoplasmic and nuclear loading control, respectively. (c) IB analysis for  $\beta$ -catenin and  $\beta$ -arr1 protein expression in nuclear extracts of CC09 cells transfected with SCR or si- $\beta$ -arr1 and treated for 30 min with ET-1 (100 nM) and/or MAC (1  $\mu$ M). Histone H3 (H3) was used as loading control. (d) Nuclear extracts of CC09 cells, treated for 30 min with ET-1 (100 nM) and/or MAC (1  $\mu$ M), were immunoprecipitated (IP) with anti- $\beta$ -arr1 or with irrelevant IgG (IgG) and immunoblotted with anti- $\beta$ -catenin and anti- $\beta$ -arr1. H3 was used as loading control. (e)  $\beta$ -catenin transcriptional activity evaluated in CC09 cells transfected with SCR or si- $\beta$ -arr1 and treated for 24 h with ET-1 (100 nM) and/or MAC (1  $\mu$ M). Values are shown as mean  $\pm$  S.D. from three independent experiments repeated in triplicates (\* $P$  < 0.001 versus CTR; \*\* $P$  < 0.002 versus ET-1 in SCR-transfected cells). (f) ET-1 promoter activity evaluated in CC09 cells treated as in (e). Values are shown as mean  $\pm$  S.D. from three independent experiments repeated in triplicates (\* $P$  < 0.001 versus CTR; \*\* $P$  < 0.001 versus ET-1 in SCR-transfected cells). ChIP analysis performed in CC09 cells treated for 30 min with ET-1 (100 nM) and/or MAC (1  $\mu$ M) (g) or in CC09 cells transfected with SCR or si- $\beta$ -arr1 and treated for 30 min with ET-1 (100 nM) and/or MAC (1  $\mu$ M) (h). Chromatin was incubated with  $\beta$ -arr1,  $\beta$ -catenin, p300, H3K27ac and TCF4 Abs and analyzed by PCR analysis by using specific primers for ET-1 promoter. Non-specific immunoglobulin G (IgG) was used as irrelevant Ab (IRR). The input DNA lane represents one-twentieth of the precleared chromatin used in each ChIP reaction. (i) ET-1, Cyclin D1 and Axin 2 mRNA expression in CC09 cells stimulated for 24 h with ET-1 (100 nM) alone or in combination with MAC (1  $\mu$ M) evaluated by qPCR, normalized using endogenous cyclophilin-A. Values are shown as mean  $\pm$  S.D. from three independent experiments repeated in triplicates (\* $P$  < 0.01 versus CTR; \*\* $P$  < 0.05 versus ET-1)

macitentan or 20% for 5-FU, for CC09 xenografts, and 83 versus 61% for macitentan or 57% for OX, for CSC5 xenografts;  $P$  < 0.05). In parallel, immunoblotting analysis of tumor xenografts of mice co-treated with macitentan and OX showed a marked effect in reducing MAPK and Akt activation, and a reversion of EMT effectors compared with controls (Figures 5b and c and Supplementary Figures S5b and c). These findings indicate that blockade of ET-1R with macitentan, in combination with chemotherapeutic drugs, controls EMT aggressive phenotype of CRC-SC, thus increasing sensitivity to the chemotherapy and promoting tumor regression.

### Discussion

The presence of stem cell-like cells has been recognized as the main cause of failure in the treatment of several

malignancies.<sup>5,6</sup> It is therefore evident that a therapeutic approach to target CSC pool could be more effective to eradicate tumor. Drug sensitivity is frequently associated with dysregulation of a signaling network rather than of a single pathway. In the present study, we provide evidence that ET-1R/ $\beta$ -arr1 links  $\beta$ -catenin signaling to sustain CRC-SC features, also through the amplification of ET-1 autocrine loop, outlining a model in which ET-1 interlinks  $\beta$ -catenin signaling to support progression and recurrence of CRC. The findings presented here reveal that ET-1R/ $\beta$ -arr1 axis has a critical role in CRC-SC signaling and chemoprotection. Notably, ET-1R blockade by macitentan markedly affected the signaling cross-talk mediated by  $\beta$ -arr1 involved in the maintenance of CRC-SC and drug response. Specifically, ET-1R blockade results in a strong decrease of survival Akt/MAPK signaling pathways,<sup>45,46</sup> with the consequent reduction of cell growth

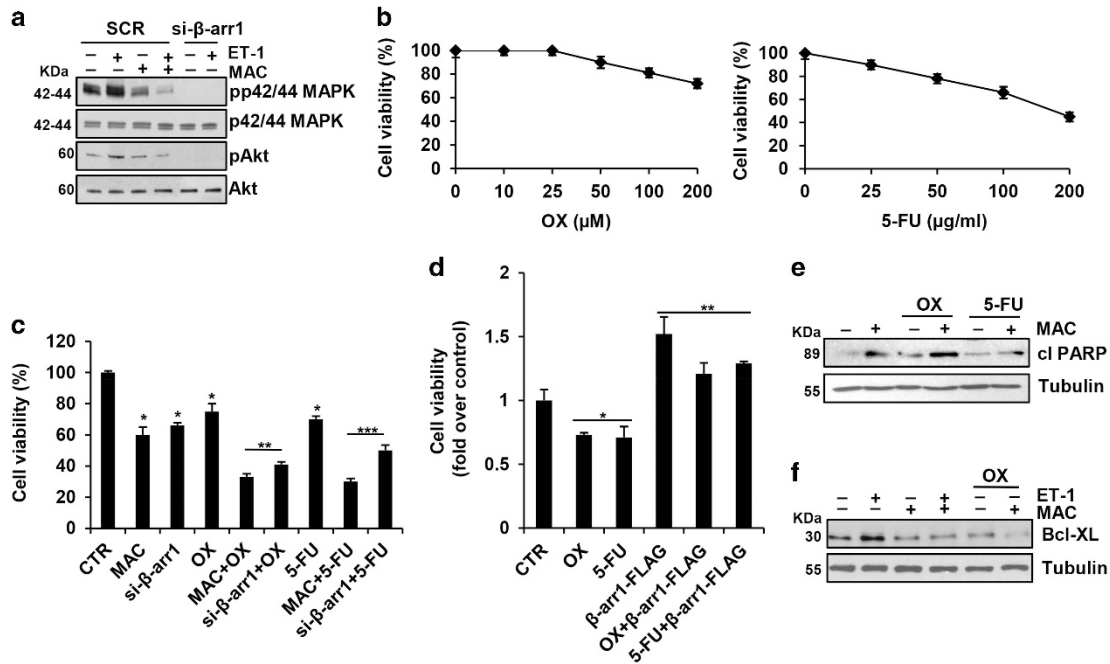


**Figure 4** ET-1R blockade sensitizes CRC-SC to standard chemotherapeutic drugs. (a) Lysates from CC09 cells treated for 1 h with ET-1 (100 nM) and/or MAC (1  $\mu$ M) and transfected with SCR or with si- $\beta$ -arr1 were immunoblotted with anti-pp42/44MAPK, anti-p42/44MAPK, anti-pAkt and anti-Akt. (b) Effect of exposure to different concentrations of oxaliplatin (OX) and 5-fluorouracil (5-FU) after 24 h on cell vitality of CC09 cells. (c) Time-dependent effect of treatment with MAC (1  $\mu$ M) or OX (100  $\mu$ M) or 5-FU (50  $\mu$ g/ml) alone and combination, for 24 h on cell growth of CC09 cells transfected with SCR or with si- $\beta$ -arr1. Values are shown as mean  $\pm$  S.D. from three independent experiments repeated in triplicates (\* $P$ <0.001 versus CTR; \*\* $P$ <0.001 versus OX; \*\*\* $P$ <0.002 versus 5-FU). (d) Effect of treatment with OX (100  $\mu$ M) or 5-FU (50  $\mu$ g/ml), for 24 h on cell growth of CC09 cells transfected with empty vector (Mock) or with  $\beta$ -arr1-FLAG. Values are shown as mean  $\pm$  S.D. from three independent experiments repeated in triplicates (\* $P$ <0.002 versus CTR; \*\* $P$ <0.002 versus chemotherapy-treated cells). (e) IB analysis of PARP cleaved form (cl PARP) in CC09 cells treated for 24 h with MAC (1  $\mu$ M) or OX (100  $\mu$ M) or 5-FU (50  $\mu$ g/ml) alone and combination. Tubulin was used as loading control. (f) IB analysis of Bcl-XL in CC09 cells treated for 24 h with ET-1 (100 nM) or MAC (1  $\mu$ M) or OX (100  $\mu$ M) alone and combination. Tubulin was used as loading control

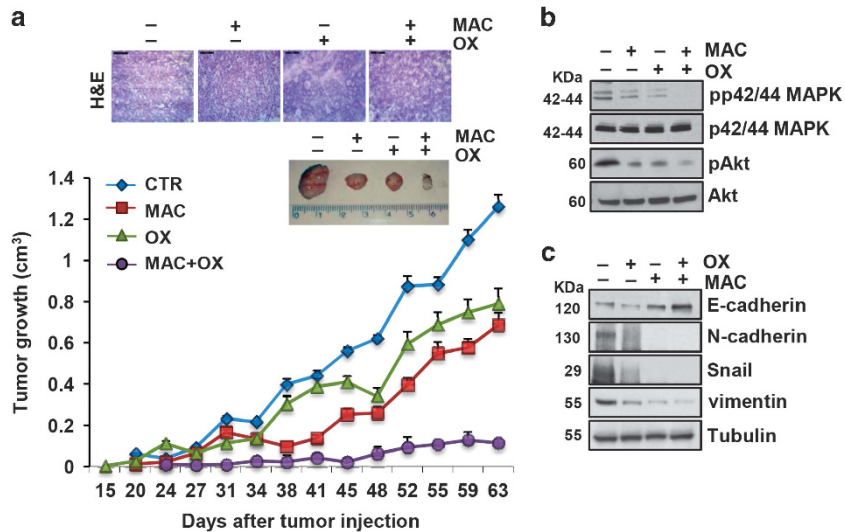


**Figure 5** ET-1R blockade by macitentan inhibits tumor growth and restores sensitivity to oxaliplatin in CRC-SC xenografts. (a) CC09 cells ( $5 \times 10^5$ ) were injected s.c. into the flank of nude mice. When tumors were detected, mice were treated with vehicle (CTR), or MAC (30 mg/Kg/oral daily), or OX (0.25 mg/Kg/i.p. once a week), or MAC (30 mg/Kg/oral daily) with OX (0.25 mg/Kg/i.p. once a week) combination for 4 weeks. The comparison of the time course of tumor growth curves by two-way ANOVA with group-by-time interaction for tumor growth was statistically significant ( $P$ <0.02). Data points, averages  $\pm$  S.D. The upper panels represented the hematoxylin–eosin staining of transplanted tumor xenografts (scale bar, 50  $\mu$ m) or the images of tumors from each treatment group. (b) Expression of pp42/44MAPK, p42/44MAPK, pAkt and Akt as evaluated by IB on total extracts from tumors of CC09 xenografts. (c) E-cadherin, N-cadherin, Snail and vimentin, evaluated by IB of total extracts from tumors of CC09 xenografts



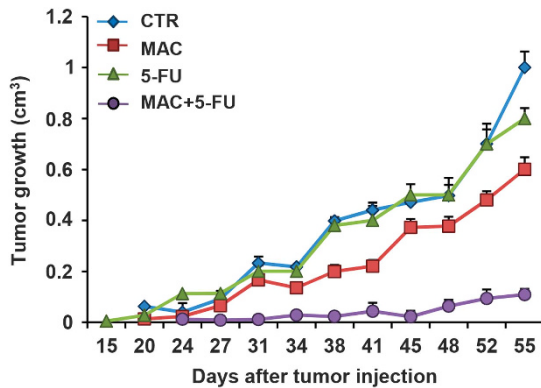


**Figure 6** Macitentan inhibits tumor growth and restores sensitivity to 5-FU in CRC-SC xenografts. CC09 cells ( $5 \times 10^5$ ) were injected s.c. into the flank of nude mice. When tumors were detected, mice were treated with vehicle (CTR), or MAC (30 mg/Kg/oral daily), or 5-FU (15 mg/Kg/i.p daily), or MAC (30 mg/Kg/oral daily) with 5-FU (15 mg/Kg/i.p daily) combination for 4 weeks. The comparison of the time course of tumor growth curves by two-way ANOVA with group-by-time interaction for tumor growth was statistically significant ( $P < 0.05$ ). Data points, averages  $\pm$  S.D.

and apoptosis induction. From a molecular standpoint, the hallmark of CRC-SC has been shown to be the abnormal activation of  $\beta$ -catenin signaling pathway and subsequent nuclear  $\beta$ -catenin accumulation.<sup>2,11–15</sup>  $\beta$ -catenin and ET-1R signaling pathways are critically involved in the progression of CRC. Our study discloses multi-point cross-talk between  $\beta$ -catenin and ET-1R/ $\beta$ -arr1 pathway in CRC-SC, indicating a promising therapeutic strategy for CRC patients. We describe the mechanistic link between ET-1 and  $\beta$ -catenin through the specific interaction with  $\beta$ -arr1. Notably,  $\beta$ -arr1 acts as a transcription co-activator that forms a complex with  $\beta$ -catenin/TCF and co-bind target genes, including ET-1. Indeed we reveal that, in response to ET-1R activation,  $\beta$ -arr1 could control two aspects of  $\beta$ -catenin nuclear functions: nuclear accumulation and assembly of a transcriptional complex. Consistent with a role of functional hub to organize nuclear complex,  $\beta$ -arr1 promotes the recruitment of p300 with TCF on ET-1 proximal promoter, and histone modification associated with ET-1 gene transcription. Macitentan interfered the functional interplay between  $\beta$ -catenin and ET<sub>A</sub>R/ $\beta$ -arr1, suppressing the transactivation of TCF4 that is essential for target gene transcription. Therefore, based on our findings, we may hypothesize that ET-1R blockade might modulate the ET-1 signaling that controls the preferences of  $\beta$ -arr1 engagement, such as  $\beta$ -catenin, which can act to convey a persistent feedback protective ET-1 autocrine loop that sustains poor drug sensitivity, EMT and invasive features.<sup>47</sup> Our data reinforce the notion that ET-1R is an important driver in CRC,<sup>17–29</sup> indicating ET-1R as novel therapeutic targets for CRC. Interestingly, ET-1R blockade by macitentan may have a dual anti-ET-1R and anti- $\beta$ -catenin activity that might be therapeutically explored. In this context, our results obtained in CRC preclinical models, indicated that macitentan, interfering with the epigenetic mechanism utilized by ET-1R/ $\beta$ -arr1 to regulate  $\beta$ -catenin-driven signaling and survival pathways, significantly improves the efficacy of OX and 5-FU-based regimens, preventing the tumor growth and increasing the sensitivity of CRC-SC to the cytotoxic agents. Much of the plasticity associated with CRC-SC arises from the local niche,

highlighting the regulatory effects of the tumor microenvironment. In this regard, the potential advantage of using the dual ET<sub>A</sub>R/ET<sub>B</sub>R antagonist macitentan is to target not only CRC, which express mainly ET<sub>A</sub>R,<sup>17–29</sup> but also tumor-associated stromal elements, such as vascular, lymphatic and inflammatory cells and fibroblasts, which all express ET<sub>B</sub>R.<sup>16,31</sup> ET<sub>B</sub>R signaling is pro-angiogenic and may also impair antitumor immunity by preventing the maturation and function of dendritic cells, which are pivotal for the initiation of T cell-mediated immune responses and the homing of T cells to tumors.<sup>48,49</sup> Therefore, the FDA approved small molecule macitentan, interfering with both ET<sub>A</sub>R and ET<sub>B</sub>R, might offer a more efficacious therapeutic strategy in combination with clinical cytotoxic drugs, because it might target aggressive CRC-SC, disabling multiple signaling circuits activated by ET<sub>A</sub>R/ $\beta$ -arr1 axis and microenvironment-associated elements expressing ET<sub>B</sub>R, offering also the opportunity to enhance antitumor immune response.<sup>50–53</sup> Of note, the cancer genome atlas (TCGA) RNAseqv2 data show high mRNA levels of ET<sub>A</sub>R, as well as of  $\beta$ -catenin, in colon adenocarcinoma samples ( $n=459$ ) compared with normal colon tissues ( $n=41$ ), as displayed with FireBrowse. The mRNA expression of ET<sub>A</sub>R and  $\beta$ -catenin was significantly upregulated in tumor samples compared with normal ( $P=1.0554e-13$  and  $P=7.3709e-11$ , respectively, as evaluated by Wilcoxon rank-sum test). We propose that high expression levels of ET<sub>A</sub>R function in CRC, at least in part, through the connection of  $\beta$ -catenin pathway. The preclinical data demonstrating that the combined treatment of macitentan and OX or 5-FU effectively reduced tumor growth suggest that CRC patients with tumor that overexpress ET<sub>A</sub>R and  $\beta$ -catenin may benefit from this combination therapy. Therefore, targeting ET-1R, empowering the  $\beta$ -catenin/ET-1 circuit, can represent a necessary measure to reach clinical efficacy for combination therapy in CRC patients. Macitentan can represent an opportunity to block connections between signaling pathways that interfere with chemotherapy drug efficacy in CRC. Our demonstration of non-canonical cross-talk between  $\beta$ -catenin and ET-1R/ $\beta$ -arr1 may have far-reaching implications in CRC and in other tumors in which ET-1R signaling is important. These data complement and add greater relevance to previous studies in ovarian,<sup>31,51–53</sup> glioblastoma,<sup>50</sup> as well as breast and lung cancer brain metastasis models,<sup>54</sup> demonstrating that, regardless of the cancer type, ET-1R might represent a vulnerability node that should be blocked to enhance sensitivity to chemotherapy. Taken together, our study identified ET-1R/ $\beta$ -arr1 as an important actionable node, demonstrating that ET-1R blockade by macitentan not only inhibits tumor growth of xenografts but also sensitizes these to chemotherapeutic agents, revealing a new prospective on the CRC patient treatment.

#### Materials and Methods

**Materials.** ET-1 was (Bachem, Bubendorf, Torrance, Switzerland) and it was used at 100 nM and incubated with the cells for the indicated times. Macitentan (MAC), also N-(5-[4-bromophenyl]-6-[2-[5-bromopyrimidin-2-yloxy]ethoxy]pyrimidin-4-yl)-N'-propylsulfamide, (Actelion Pharmaceuticals, Allschwil, Switzerland). Pre-treatment of cells with MAC, was used at the concentration of 1  $\mu$ M for 30 min prior to the addition of ET-1. Oxaliplatin (SUN PHARMA, Goregaon (E), Mumbai) used at 100  $\mu$ M and Fluorouracil (5-FU) (TEVA, Petach Tikva, Israel), used at 50  $\mu$ g/ml.

**Cell culture.** The patient-derived CRC-SC enriched cultures (CC09, CSC5, CSC2 and CSC1), isolated from human tumor samples and capable to reproduce a histological copy of the original patient tumor when inoculated in immunocompromised mice, were kindly provided by the Istituto Superiore di Sanità (ISS) CSC biobank.<sup>3,10,12</sup> Cells were cultured in ultra-low attachment plates and maintained in stem cell medium (DMEM/F12, supplemented as reported in ref. 10) and monthly tested for mycoplasma contamination. Genomic analysis of CRC-SC showed that CC09 carried mutant BRAF, PIK3CA, APC, TP53 and SMAD4; CSC5 carried mutant KRAS, PIK3CA, APC and SMAD4; CSC2 carried mutant KRAS, APC, TP53 and SMAD4; CSC1 carried mutant PIK3CA, APC and SMAD4 (ref. 3) and unpublished results.

**Immunoblotting analysis.** Whole-cell lysates of CRC-SC were prepared using an ice-cold modified RIPA buffer (50 mM Tris-HCl pH 7.4, 250 mM NaCl, 1% Triton X-100, 1% sodium deoxycholate, 0.1% SDS) containing a mixture of protease and phosphatase inhibitors or NE-PER nuclear and cytoplasmic extraction reagents (Thermo Fisher Scientific, Waltham, USA) to separate cytoplasmic and nuclear fractions. Protein content of the extracts was determined using protein assay kit (Bio-Rad, Hercules, CA, USA) and resolved by SDS-PAGE. Immunoblotting of Abs specific for  $\beta$ -arr1 (K-16: sc-9182),  $\beta$ -Catenin (E-5: sc-7963), tubulin (DM1A: sc-32293), MMP-2 (K-20: sc-8835), MMP-9 (M-17: sc-6841), Snail (E-18: sc-10432), vimentin (C-20: sc-7557), Histone H3 (C-16: sc-8654), PCNA (F-2: sc-25280), (Santa Cruz Biotechnology Dallas, TX, USA), HSP-70 (Enzo Life Sciences, New York, USA, ADI-SPA-812), Twist (ab50581), ET<sub>A</sub>R (ab178454), ET<sub>B</sub>R (ab39960) (Abcam, Cambridge, UK), AKT (9272) pAKT (Ser-473) (9271), p44/42MAPK (9102), pp42/44MAPK (4377), cleaved-PARP (9541), non-phospho (active)  $\beta$ -Catenin (Ser33/37/Thr41) (4270) (Cell Signaling, Beverly, MA, USA), N-cadherin (610920), E-cadherin (610181) (BD Biosciences, Franklin Lakes, NJ, USA) were detected using HRP-conjugated anti-mouse or anti-rabbit Abs (Pierce, 31460) and visualized by enhanced chemiluminescence detection system (ECL, Bio-Rad).

**Immunoprecipitation analysis.** Nuclear extracts were immunoprecipitated as previously described,<sup>31</sup> using  $\beta$ -arr1, or non-specific immunoglobulin G (IgG) (Santa Cruz Biotechnology) and protein G-agarose beads (Thermo Fisher Scientific) at 4 °C overnight. Immunoprecipitates were resolved by SDS-PAGE and the proteins were detected by IB with the following Abs:  $\beta$ -Catenin,  $\beta$ -arr1 and Histone 3 (Santa Cruz Biotechnology). To obtain clean and specific IB signals of  $\beta$ -arr1 which run very close to heavy chain of IgG, we used HRP-conjugated protein A (Thermo Scientific, Waltham, MA, USA) instead of HRP-conjugated secondary Ab.

**RNA silencing and transfection.** For the silencing of  $\beta$ -arr1, the CRC-SC were transiently transfected with ON-TARGET plus Human ARRB1 siRNA-SMART pool, containing four different siRNAs targeting  $\beta$ -arr1 (Dharmacon, Lafayette, CO, USA). The ON-TARGET plus Control Non-targeting siRNA (Dharmacon) was used as negative control. For exogenous expression of  $\beta$ -arr1 we used pcDNA3- $\beta$ -arr1-FLAG (wild-type) plasmid vector, containing a 'wobble' mutant construct encoding rat  $\beta$ -arr1 sequences resistant to small interfering RNA targeting, kindly provided by Dr. Robert Lefkowitz (Howard Hughes Medical Institute, Duke University, Durham, NC, USA). Cells transfected with the empty vector pcDNA3 were used as negative control (Mock).

**RNA isolation and qPCR.** Total RNA was isolated using Trizol (Thermo Fisher Scientific) according to the manufacturer's protocol. RNA was reversed transcribed using Super Script VIL0 cDNA synthesis kit (Thermo Fisher Scientific). Quantitative real-time PCR (qPCR) was performed by using LightCycler rapid thermal cycler system (Roche Diagnostics, Basel, Switzerland) and 7500 Fast real-time PCR System (Thermo Fisher Scientific). The expression levels of mRNA were determined by normalizing to cyclophilin-A mRNA expression. Each PCR analysis was done twice separately. Final data were obtained by using 2<sup>- $\Delta\Delta$ Ct</sup> method. The primers sets used were as follows: ET-1 F: CACCGAATTCGAATGTGAC and ET-1R: 5'-TCCTCTGCTGGTTCCTGACT-3'; ET<sub>A</sub>R F: 5'-GTCTGCTGTGGGCA ATAGTTG-3' and ET<sub>A</sub>R R: 5'-GCTTCTGTTTACCACCTCATCAA-3'; ET<sub>B</sub>R F: 5'-TCCCCTTCAAGAAGACAGCTT-3' and ET<sub>B</sub>R R: 5'-CAGAGGGCAAGACAAGGAC-3';  $\beta$ -arr1 F: 5'-CAGTATGCAGACATGCGCTTT-3' and  $\beta$ -arr1 R: 5'-AGTTCTGTCTTCTGCTGCT-3'; E-cadherin F: 5'-CCCACCCAGTACAAGGTC-3' and E-cadherin R: 5'-ATGCCATCGTTGTTCACTGGA-3'; N-cadherin F: 5'-GGTGGAG GAGAAGAAGACCAG-3' and N-cadherin R: 5'-GGCATCAGGCTCCACAGT-3'; Snail F: 5'-CACTATGCCGCGCTCTTTCC-3' and Snail R: 5'-GTCGTAGGGCTGTGGAAG-3'; Axin 2 F: 5'-CTGGCTTTGGTGAATGTTG-3' and Axin 2R: 5'-CTGG

CTTTGGTGAAGTGTG-3'; Cyclin D1 F: 5'-CTAATGGAATGGTTTGGGAATATCC ATGTA-3' and Cyclin D1 R: 5'-AAAGGAAGTATCATCCTGGCAAT-3'; Cyclophilin-A F: 5'-TTCATCTGCACTGCCAAGAC-3' and Cyclophilin-A R: 5'-TCGAGTTGTCCA CAGTCAGC-3'.

**Chromatin immunoprecipitation.** Chromatin was extracted from CRC-SC cells ( $5 \times 10^6$ ) and ChIP assays were performed as previously described.<sup>31</sup> The differential binding between proteins and promoter DNA was examined by PCR. The primary Abs used were as follows: anti- $\beta$ -catenin (E-5: sc-7963), anti- $\beta$ -arr1 (K-16: sc-9182), anti-p300 (N-15: sc-584), TCF4 (H-125: sc-13027) (Santa Cruz Biotechnology) anti-acetylated Histone H3 (Lys 27) (Millipore, Billerica, MA, USA, 07-360). The primers used were as follows: ET-1 promoter 5'-CAGCTTGCAA AGGGGAAGCG-3' and 5'-TCCGACTTTATCCAGCCCC-3'.

**Luciferase reporter gene assay.** The CRC-SC were transiently transfected, using Lipofectamine 2000 (Thermo Fisher Scientific) according to manufacturer's instructions, with pGL3-SNA (-869/+59) construct (kindly provided by Dr. A. Garcia de Herreros, Institut Municipal d'Investigació Mèdica, Universitat Pompeu Fabra, Barcelona, Spain) or with pGL2-Ecad3 construct (kindly provided by Dr. E.R. Fearon, University of Michigan, Ann Arbor, MI, USA), respectively containing luciferase gene under the control of the human Snail and E-cadherin promoter, and with pCMV- $\beta$ -galactosidase vector (Promega, Madison, WI, USA). Transcriptional activity of  $\beta$ -catenin/TCF was evaluated by transient transfection of CRC-SC with TOP/Flash luciferase reporter, containing multiple TCF4 binding sites for  $\beta$ -catenin and FOP/Flash luciferase reporter (negative control) (results were expressed as the ratio of TOP/Flash over FOP/Flash activity) and pCMV- $\beta$ -galactosidase vector. To measure the ET-1 promoter activity, the human CRC-SC, were transiently co-transfected with ET-1 promoter reporter sequence, spanning -1300 to +230 bp surrounding the transcriptional initiation site and containing a functional TBE located at -73 to -67 bp, kindly provided by Dr. Z. Zhang (University of California San Diego School of Medicine, La Jolla, CA, USA), and pCMV- $\beta$ -galactosidase vector. Reporter activity was measured using the Luciferase assay system (Promega) and normalized to  $\beta$ -galactosidase activity.

**Gelatin zymography.** To detect MMP-9 and -2 activity in conditioned media, CRC-SC transiently transfected with si- $\beta$ -arr1 or with negative control, were stimulated with ET-1 or MAC, alone or in combination for 24 h. Conditioned media was collected and concentrated by using Spin-X UF concentrator columns (Corning, New York, NY, USA). Conditioned medium was separated by 9% SDS-PAGE gels containing 1 mg/ml gelatin. The gels were washed for 30 min at 22 °C in 2.5% Triton X-100 and then incubated in 50 mM Tris (pH 7.6), 1 mM ZnCl<sub>2</sub>, and 5 mM CaCl<sub>2</sub> for 18 h at 37 °C. After incubation the gels were stained with 0.2% Coomassie Blue. Enzyme-digested regions were identified as white bands on a blue background and quantified by computerized image analysis of the band. Molecular sizes were determined from the mobility, using gelatin zymography standards (Bio-Rad Laboratories, Richmond, CA, USA).

**Invasion assay.** Chemoinvasion assays were carried out using modified Boyden Chambers consisting of transwell membrane filter inserts with 8  $\mu$ m size polycarbonate membrane precoated with polymerized collagen placed in a 24-well plate (BD Biosciences). The human CRC-SC clones transiently transfected with si- $\beta$ -arr1 or with negative control, were stimulated with ET-1 or MAC, alone or in combination with ET-1, added to the lower chamber. The cells were left to migrate for 24 h at 37 °C. Cells on the upper part of the membrane were scraped using a cotton swab and the migrated cells were stained using Diff-Quick kit (Merz-Dade). The experiment was performed in triplicates for all conditions described. From every transwell, several images were taken under a phase-contrast microscope at  $\times 10$  magnification and two broad fields were considered for quantification. The results of the analysis of the individual photos are depicted as dots in the various graphs, normalized to control and shown as fold of control.

**ELISA.** The release of ET-1 in media of CRC-SC was measured in triplicate on microtiter plates by using an ELISA kit (Phoenix Pharmaceuticals, Burlingame, CA, USA) according to the manufacturer's instructions.

**Cell viability analysis.** The human CRC-SC were seeded in triplicates, in 24-well plates. The cells were transiently transfected with si- $\beta$ -arr1 or  $\beta$ -arr1-FLAG or with specific negative control and treated with ET-1, MAC, OX and 5-FU, alone or in combination. After 24 or 48 or 72 h cell viability was determined by counting the



cells, for each time point, using a Neubauer-counting chamber and a bright field microscope. The trypan blue dye exclusion method was used to evaluate the percentage of viable cells.

**Clonogenic assay.** The CRC-SC tumor spheres were mechanically dissociated and the resulting cells were seeded at low densities (1000 cells/ml) in 12-well low adhesion plates at 1 ml per well, in stemness medium with or without ET-1 or MAC, alone or in combination. After 7 days of growth, the tumor spheres obtained were analyzed and quantified by a phase-contrast microscope at  $\times 10$  magnification.

**CRC-SC xenografts.** Athymic ( $\text{nu}^+/\text{nu}^+$ ) mice, 5- to 6-week of age (Charles River Laboratories, Milan, Italy), were subcutaneously injected with  $5 \times 10^5$  viable CRC-SC, in 100  $\mu\text{l}$  PBS/Matrigel (BD Biosciences) into the flank, following the guidelines of the Italian Ministry of Health. For all the CRC-SC, xenografts were detectable within 2–6 weeks. Tumor xenografts were extracted, formalin-fixed, and paraffin-embedded. Haematoxylin–eosin-stained sections were subsequently evaluated by a pathologist in comparison with human tumors. For drug testing,  $5 \times 10^5$  viable CRC-SC, in 100  $\mu\text{l}$  PBS/Matrigel, were subcutaneously injected into the flank of mice and were allowed to grow until they reached a detectable size. Drug treatments were started when tumors were detected, mice were randomized into different groups of 10 mice undergoing the following treatments for 4 weeks: (i) vehicle (control), (ii) macitentan (30 mg/Kg/oral daily), (iii) OX (0.25 mg/Kg/i.p. once a week) or 5-FU (15 mg/Kg/i.p. daily), (iv) macitentan plus OX or 5-FU. Tumor volume was measured with caliper and the tumor growth curves were plotted. Tumor volume was calculated using the formula:  $\pi/6$  larger diameter  $\times$  (smaller diameter)<sup>2</sup>. At the end of experiments all mice were euthanized and tumors were harvested and preserved for further analysis.

**Statistical analysis.** Statistical analysis was performed using Student's *t*-test and Fisher's exact test to compare *in vitro* experiments. The time course of tumor growth was compared across the groups using two-way ANOVA, with group and time as variables. All statistical tests were carried out using SPSS software (SPSS 11, SPSS Inc. Chicago, IL, USA). A two-sided probability value of  $< 0.05$  was considered statistically significant. The Wilcoxon rank-sum test was used to analyze the gene expression obtained from TCGA of colon adenocarcinoma samples.

## Conflict of Interest

The authors declare no conflict of interest.

**Acknowledgements.** We gratefully acknowledge Aldo Lupo for technical assistance and Maria Vincenza Sarcone for secretarial support. This work was supported by the Italian Association for Cancer Research (AIRC) (AIRC18382 to AB) and AIRC 5  $\times$  1000 (9979 to RDM).

- Walker AS, Johnson EK, Maykel JA, Stojadinovic A, Nissán A, Brucher B *et al*. Future directions for the early detection of colorectal cancer recurrence. *J Cancer* 2014; **5**: 272–280.
- Clevers H. Wnt/ $\beta$ -catenin signaling in development and disease. *Cell* 2006; **127**: 469–480.
- De Angelis ML, Zeuner A, Policicchio E, Russo G, Bruselles A, Signore M *et al*. Cancer stem cell-based models of colorectal cancer reveal molecular determinants of therapy resistance. *Stem Cell Transl Med* 2016; **5**: 511–523.
- Zeuner A, Todaro M, Stassi G, De Maria R. Colorectal cancer stem cells: from the crypt to the clinic. *Cell Stem Cell* 2014; **15**: 692–705.
- Colak S, Medema JP. Cancer stem cells—important players in tumor therapy resistance. *FEBS J* 2014; **281**: 4779–4791.
- Kemper K, Grandela C, Medema JP. Molecular identification and targeting of colorectal cancer stem cells. *Oncotarget* 2010; **1**: 387–395.
- Todaro M, Francipane MG, Medema JP, Stassi G. Colon cancer stem cells: promise of targeted therapy. *Gastroenterology* 2010; **138**: 2151–2162.
- Vermeulen L, Sprick MR, Kemper K, Stassi G, Medema JP. Cancer stem cells: old concepts, new insights. *Cell Death Differ* 2008; **15**: 947–958.
- Ricci-Vitiani L, Lombardi DG, Pilozzi E, Biffoni M, Todaro M, Peschle C *et al*. Identification and expansion of human colon-cancer-initiating cells. *Nature* 2007; **445**: 111–115.
- Todaro M, Alea MP, Di Stefano AB, Cammareri P, Vermeulen L, Iovino F *et al*. Colon cancer stem cells dictate tumor growth and resist cell death by production of interleukin-4. *Cell Stem Cell* 2007; **1**: 389–402.

- Francescangeli F, Contavalli P, De Angelis L, Baiocchi M, Gambarà G, Pagliuca A *et al*. Dynamic regulation of the cancer stem cell compartment by Cripto-1 in colorectal cancer. *Cell Death Differ* 2015; **22**: 1700–1713.
- Todaro M, Gaggianesi M, Catalano V, Benfante A, Iovino F, Biffoni M *et al*. CD44v6 is a marker of constitutive and reprogrammed cancer stem cells driving colon cancer metastasis. *Cell Stem Cell* 2014; **14**: 342–356.
- de Sousa EM, Vermeulen L, Richel D, Medema JP. Targeting Wnt signaling in colon cancer stem cells. *Clin Cancer Res* 2011; **17**: 647–653.
- Kanwar S, Yu Y, Nautiyal J, Patel B, Majumdar A. The Wnt/ $\beta$ -atenin pathway regulates growth and maintenance of colonospheres. *Mol Cancer* 2010; **9**: 212–225.
- Clevers H, Loh KM, Nusse R. Stem cell signaling. An integral program for tissue renewal and regeneration: Wnt signaling and stem cell control. *Science* 2014; **346**: 1248012–1248019.
- Rosano L, Spinella F, Bagnato A. Endothelin 1 in cancer: biological implications and therapeutic opportunities. *Nat Rev Cancer* 2013; **13**: 637–651.
- Wang Z, Liu P, Zhou X, Wang T, Feng X, Sun YP *et al*. Endothelin promotes colorectal tumorigenesis by activating YAP/TAZ. *Cancer Res* 2017; **77**: 2413–2423.
- Liakou P, Tepetes K, Germentis A, Leventaki V, Atsaves V, Patsouris E *et al*. Expression patterns of endothelin-1 and its receptors in colorectal cancer. *J Surg Oncol* 2012; **105**: 643–649.
- Arun C, London NJ, Hemingway DM. Prognostic significance of elevated endothelin-1 levels in patients with colorectal cancer. *Int J Biol Markers* 2004; **19**: 32–37.
- Nie S, Zhou J, Bai F, Jiang B, Chen J, Zhou J. Role of endothelin A receptor in colon cancer metastasis: *in vitro* and *in vivo* evidence. *Mol Carcinog* 2014; **53**: E85–E91.
- Hoossein MM, Dashwood MR, Dawas K, Ali HM, Grant K, Savage F *et al*. Altered endothelin receptor subtypes in colorectal cancer. *Eur J Gastroenterol Hepatol* 2007; **19**: 775–782.
- Ali H, Dashwood M, Dawas K, Loizidou M, Savage F, Taylor I. Endothelin Receptor expression in colorectal cancer. *J Cardiovasc Pharmacol* 2000; **36**: S69–S71.
- Ali H, Loizidou M, Dashwood M, Savage F, Sheard C, Taylor I. Stimulation of colorectal cancer cell line growth by ET-1 and its inhibition by ET(A) antagonists. *Gut* 2000; **47**: 685–688.
- Chen C, Wang L, Liao Q, Huang Y, Ye H, Chen F *et al*. Hypermethylation of EDNRB promoter contributes to the risk of colorectal cancer. *Diagn Pathol* 2013; **10**: 199–205.
- Aslam E, Shankar A, Loizidou M, Fredericks S, Miller K, Boulos PB *et al*. Increased endothelin-1 in colorectal cancer and reduction of tumor growth by ET(A) receptor antagonism. *Br J Cancer* 2001; **85**: 1759–1763.
- Shankar A, Loizidou M, Aliex G, Fredericks S, Holt D, Boulos PB *et al*. Raised endothelin 1 levels in patient with colorectal liver metastases. *Br J Surg* 1998; **85**: 502–506.
- Kim TH, Xiong H, Zhang Z, Ren B.  $\beta$ -catenin activates the growth factor endothelin-1 in colon cancer cells. *Oncogene* 2005; **24**: 597–604.
- Puglisi MA, Barba M, Corbi M, Errico MF, Giorda E, Saulnier N *et al*. Identification of Endothelin-1 and NR4A2 as CD133-regulated genes in colon cancer cells. *J Pathol* 2011; **225**: 305–314.
- Haque SU, Dashwood MR, Heetun M, Shiwen X, Farooqui N, Ramesh B *et al*. Efficacy of the specific endothelin A receptor antagonist zibotentan (ZD4054) in colorectal cancer: a preclinical study. *Mol Cancer Ther* 2013; **12**: 1556–1567.
- Bhattacharya B, Low SH, Chong ML, Chia D, Koh KX, Sapari NS *et al*. Acquired resistance to combination treatment through loss of synergy with MEK and PI3K inhibitors in colorectal cancer. *Oncotarget* 2016; **7**: 29187–29198.
- Rosano L, Cianfrocca R, Tocci P, Spinella F, Di Castro V, Caparra V *et al*. Endothelin A receptor/ $\beta$ -Arrestin signaling to the Wnt pathway renders ovarian cancer cells resistant to chemotherapy. *Cancer Res* 2014; **74**: 7453–7464.
- Rosano L, Cianfrocca R, Tocci P, Spinella F, Di Castro V, Spadaro F *et al*.  $\beta$ -arrestin-1 is a nuclear transcriptional regulator of endothelin-1-induced  $\beta$ -catenin signalling. *Oncogene* 2013; **32**: 5066–5077.
- Rosano L, Cianfrocca R, Spinella F, Di Castro V, Nicotra MR, Lucidi A *et al*. Acquisition of chemoresistance and EMT phenotype is linked with activation of the endothelin A receptor pathway in ovarian carcinoma cells. *Clin Cancer Res* 2011; **17**: 2350–2360.
- Rosano L, Bagnato A. Convergent pathways link the endothelin A receptor to the  $\beta$ -catenin: the  $\beta$ -arrestin connection. *Cell Cycle* 2009; **8**: 1462–1463.
- Rosano L, Cianfrocca R, Masi S, Spinella F, Di Castro V, Bircocci A *et al*.  $\beta$ -arrestin links endothelin A receptor to  $\beta$ -catenin signaling to induce ovarian cancer cell invasion and metastasis. *Proc Natl Acad Sci* 2009; **106**: 2806–2811.
- Soh B, Ng SY, Wu H, Buac K, Park JH, Lian X *et al*. Endothelin-1 supports clonal derivation and expansion of cardiovascular progenitors derived from human embryonic stem cells. *Nat Commun* 2016; **7**: 10774.
- Zhan Y, Xu C, Liu Z, Yang Y, Tan S, Yang Y *et al*.  $\beta$ -Arrestin1 inhibits chemotherapy-induced intestinal stem cell apoptosis and mucositis. *Cell Death Dis* 2016; **7**: e2229.
- Bagnato A, Salani D, Di Castro V, Wu-Wong JR, Tecce R, Nicotra MR *et al*. Expression of endothelin 1 and endothelin A receptor in ovarian carcinoma: evidence for an autocrine role in tumor growth. *Cancer Res* 1999; **59**: 720–727.
- Pereira L, Mariadason JM, Hannan RD, Dhillon AS. Implications of epithelial-mesenchymal plasticity for heterogeneity in colorectal cancer. *Front Oncol* 2015; **5**: 13 eCollection 2015.
- Han XY, Wei B, Fang JF, Zhang S, Zhang FC, Zhang HB *et al*. Epithelial-mesenchymal transition associates with maintenance of stemness in spheroid-derived stem-like colon cancer cells. *PLoS One* 2013; **8**: e73341.

41. Li J, Zhou BP. Activation of  $\beta$ -catenin and Akt pathways by Twist are critical for the maintenance of EMT associated cancer stem cell-like characters. *BMC Cancer* 2011; **11**: 49.
42. Polyak K, Weinberg RA. Transitions between epithelial and mesenchymal states: acquisition of malignant and stem cell traits. *Nat Rev Cancer* 2009; **9**: 265–273.
43. Mani SA, Guo W, Liao MJ, Eaton EN, Ayyanan A, Zhou AY *et al*. The epithelial-mesenchymal transition generates cells with properties of stem cells. *Cell* 2008; **133**: 704–715.
44. Brabletz T, Hlubek F, Spaderna S, Schmalhofer O, Hiendlmeyer E, Jung A *et al*. Invasion and metastasis in colorectal cancer: epithelial-mesenchymal transition, mesenchymal-epithelial transition, stem cells and beta-catenin. *Cells Tissues Organs* 2005; **179**: 56–65.
45. Wang YK1, Zhu YL, Qiu FM, Zhang T, Chen ZG, Zheng S *et al*. Activation of Akt and MAPK pathways enhances the tumorigenicity of CD133+ primary colon cancer cells. *Carcinogenesis* 2010; **31**: 1376–1380.
46. Catalano V, Dentice M, Ambrosio R, Luongo C, Carollo R, Benfante A *et al*. Activated thyroid hormone promotes differentiation and chemotherapeutic sensitization of colorectal cancer stem cells by regulating Wnt and BMP4 signaling. *Cancer Res* 2016; **76**: 1237–1244.
47. Rosanò L, Bagnato A.  $\beta$ -arrestin1 at the cross-road of endothelin-1 signaling in cancer. *J Exp Clin Cancer Res* 2016; **35**: 121–132.
48. Buckanovich RJ, Facciabene A, Kim S, Benencia F, Sasaroli D, Balint K *et al*. Endothelin B receptor mediates the endothelial barrier to T cell homing to tumors and disables immune therapy. *Nat Med* 2008; **14**: 28–36.
49. Kandalafi LE, Facciabene A, Buckanovich RJ, Coukos G. Endothelin B receptor, a new target in cancer immune therapy. *Clin Cancer Res* 2009; **15**: 4521–4528.
50. Kim SJ, Lee HJ, Kim MS, Choi HJ, He J, Wu Q *et al*. Macitentan, a dual endothelin receptor antagonist, in combination with temozolomide leads to glioblastoma regression and long-term survival in mice. *Clin Cancer Res* 2015; **21**: 4630–4641.
51. Coffman L, Mooney C, Lim J, Bai S, Silva I, Gong Y *et al*. Endothelin receptor-A is required for the recruitment of antitumor T cells and modulates chemotherapy induction of cancer stem cells. *Cancer Biol Ther* 2013; **14**: 184–192.
52. Kim SJ, Kim JS, Kim SW, Yun SJ, He J, Brantley E *et al*. Antivascular therapy for multidrug-resistant ovarian tumors by macitentan, a dual endothelin receptor antagonist. *Transl Oncol* 2012; **5**: 39–47.
53. Kim SJ, Kim JS, Kim SW, Brantley E, Yun SJ, He J *et al*. Macitentan (ACT-064992), a tissue-targeting endothelin receptor antagonist, enhances therapeutic efficacy of Paclitaxel by modulating survival pathways in orthotopic models of metastatic human ovarian cancer. *Neoplasia* 2011; **13**: 167–179.
54. Lee HJ, Hanibuchi M, Kim SJ, Yu H, Kim MS, He J *et al*. Treatment of experimental human breast cancer and lung cancer brain metastases in mice by macitentan, a dual antagonist of endothelin receptors, combined with paclitaxel. *Neuro Oncol* 2016; **18**: 486–496.



This work is licensed under a Creative Commons Attribution-NonCommercial-NoDerivs 4.0 International License. The images or other third party material in this article are included in the article's Creative Commons license, unless indicated otherwise in the credit line; if the material is not included under the Creative Commons license, users will need to obtain permission from the license holder to reproduce the material. To view a copy of this license, visit <http://creativecommons.org/licenses/by-nc-nd/4.0/>

© The Author(s) 2017

Supplementary Information accompanies this paper on Cell Death and Differentiation website (<http://www.nature.com/cdd>)